





Fluorescence evidence of annexin A6 translocation across membrane in model matrix vesicles during apatite formation

Yubo Wang^{1,2} | Liliana Weremiejczyk³ | Agnieszka Strzelecka-Kiliszek³ | Ofelia Maniti¹  |
 Ekeveliny Amabile Veschi⁴ | Mayte Bolean⁴ | Ana Paula Ramos⁴ | Layth Ben Trad¹  |
 David Magne¹ | Joanna Bandorowicz-Pikula⁵ | Slawomir Pikula³ | Jose Luis Millán⁶ |
 Massimo Bottini⁷  | Peter Goekjian¹ | Pietro Ciancaglini⁴ | René Buchet¹  |
 Wei Tao Dou² | He Tian² | Saïda Mebarek¹ | Xiao P. He² | Thierry Granjon¹

¹Univ LyonUCBL, CNRS, ICBMS UMR 5246, IMBL, Lyon, France

²Key Laboratory for Advanced Materials and Joint International Research Laboratory of Precision Chemistry and Molecular Engineering, Feringa Nobel Prize Scientist Joint Research Centre, East China University of Science and Technology, Shanghai, China

³Laboratory of Biochemistry of Lipids, Nencki Institute of Experimental Biology, Warsaw, Poland

⁴Departamento de Química, Faculdade de Filosofia, Ciências e Letras de Ribeirão Preto da Universidade de São Paulo (FFCLRP-USP) Ribeirão Preto, São Paulo, Brazil

⁵Laboratory of Cellular Metabolism, Nencki Institute of Experimental Biology, Warsaw, Poland

⁶Sanford Burnham Prebys Medical Discovery Institute, La Jolla, California, USA

⁷Department of Experimental Medicine, University of Rome Tor Vergata, Rome, Italy

Correspondence

Thierry Granjon, ICBMS UMR-CNRS 5246, Bat. LEDERER, 1 rue Victor GRIGNARD, Université Lyon 1 - F-69622 Villeurbanne cedex, France.
 Email: thierry.granjon@univ-lyon1.fr

Abstract

Matrix vesicles (MVs) are 100–300 nm spherical structures released by mineralization competent cells to initiate formation of apatite, the mineral component in bones. Among proteins present in MVs, annexin A6 (AnxA6) is thought to be ubiquitously distributed in the MVs' lumen, on the surface of the internal and external leaflets of the membrane and also inserted in the lipid bilayer. To determine the molecular mechanism(s) that lead to the different locations of AnxA6, we hypothesized the occurrence of a pH drop during the mineralization. Such a change would induce the AnxA6 protonation, which in turn, and because of its isoelectric point of 5.41, would change the protein hydrophobicity facilitating its insertion into the MVs' bilayer. The various distributions of AnxA6 are likely to disturb membrane phospholipid organization. To examine this possibility, we used fluorescein as pH reporter, and established that pH decreased inside MVs during apatite formation. Then, 4-(14-phenyldibenzo[a,c]phenazin-9(14H)-yl)-phenol, a vibration-induced emission fluorescent probe, was used as a reporter of changes in membrane organization occurring with the varying mode of AnxA6 binding. Proteoliposomes containing AnxA6 and 1,2-Dimyristoyl-*sn*-glycero-3-phosphocholine (DMPC) or 1,2-Dimyristoyl-*sn*-glycero-3-phosphocholine: 1,2-Dipalmitoyl-*sn*-glycero-3-phosphoserine (DMPC:DPPS 9:1), to mimic the external and internal MV membrane leaflet, respectively, served as biomimetic models to investigate the nature of AnxA6 binding. Addition of Anx6 to DMPC at pH 7.4 and 5.4, or DMPC:DPPS (9:1) at pH 7.4 induced a decrease in membrane fluidity, consistent with AnxA6 interactions with the bilayer surface. In contrast, AnxA6 addition to DMPC:DPPS (9:1) at pH 5.4 increased the fluidity of the membrane. This latest result was interpreted as reflecting the insertion of AnxA6 into the bilayer. Taken together, these findings point to a possible mechanism of AnxA6 translocation in MVs from the surface of the internal leaflet into the phospholipid bilayer stimulated upon acidification of the MVs' lumen during formation of apatite.

KEYWORDS

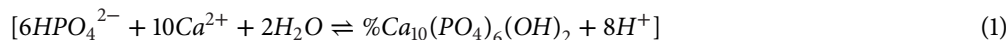
annexin A6, apatite, chondrocyte, fluidity, fluorescence, matrix vesicles, osteoblast, proteoliposome, translocation

This is an open access article under the terms of the [Creative Commons Attribution-NonCommercial-NoDerivs License](https://creativecommons.org/licenses/by-nc-nd/4.0/), which permits use and distribution in any medium, provided the original work is properly cited, the use is non-commercial and no modifications or adaptations are made.

© 2022 The Authors. *Journal of Extracellular Biology* published by Wiley Periodicals, LLC on behalf of the International Society for Extracellular Vesicles.

1 | INTRODUCTION

Biom mineralization is a highly regulated process that takes place during the formation, development, remodelling and repair of skeletal tissues (Blair et al., 2002; Raggatt & Partridge, 2010). Skeletal formation is a complex process that involves osteoblasts during transmembranous ossification and chondrocytes during endochondral ossification (Berendsen & Olsen, 2015; Hallett et al., 2019). Both osteoblasts and chondrocytes are able to release matrix vesicles (MVs), 100–300 nm diameter spherical structures enriched in proteins associated with the initiation of mineralization (Anderson, 2003; Bottini et al., 2018; Golub, 2009; Wuthier et al., 2011). Calcium (~1–2 mM) and phosphate (~1–2 mM) concentrations are in supersaturation under physiological conditions and promote apatite formation (Boskey et al., 1982; Kuhn et al., 2000) with release of protons (Equation 1) (Smith et al., 2005; Tye et al., 2010).



Protons are released during apatite formation at biological pH due to the deprotonation of the monobasic H_2PO_4^- or dibasic HPO_4^{2-} . Approximately 4–8 protons from monobasic phosphate and up to 14 protons from dibasic phosphate are released per apatite, $\text{Ca}_{10-x}(\text{HPO}_4)_v(\text{CO}_3)_w(\text{PO}_4)_{6-x}(\text{OH})_{2-x}$, depending of the exact amount of acidic phosphate precursor (v) and carbonate (w) with $x = v+w$ (Aoba & Moreno, 1992; Simmer & Fincham, 1995; Smith et al., 2005). Although the calcium and phosphate ionic concentrations are sufficient to spontaneously initiate formation of calcium phosphate complexes, nucleation speeds up formation of apatite crystals (Veis & Dorvee, 2013), while mineralization inhibitors maintain driving forces for calcium phosphate precipitation and prevent unwanted pathological mineralization (Margolis et al., 2014). Among the MV-associated proteins, the annexin (Anx) family members are the most abundant (Bottini et al., 2018; Genge et al., 2007). Annexins are calcium- and phospholipid-binding proteins (Bandorowicz & Pikuła, 1993; Bandorowicz-Pikuła & Pikuła, 1998; Cornely et al., 2011; Gerke & Moss, 2002; Smith et al., 1994). AnxA6, which is the largest member of the Anx family (MW of ~68 kDa) (Cornely et al., 2011; Smith et al., 1994), binds in a Ca^{2+} dependent manner to negatively charged phospholipids such as phosphatidylserine which is localized on the inner leaflet of the MVs' lipid bilayer. AnxA6 was found to exist in the MV membrane as both an integral and a peripheral protein, which suggests distinct lipid-protein interactions and possible functions (Kirsch et al., 2000; Veschi et al., 2020). A population of AnxA6 was found to be bound to the internal leaflet of MVs, another part of AnxA6 remains inserted in the membrane, as well as attached to the external leaflet (Veschi et al., 2020). It was hypothesized that during apatite formation in the MVs' lumen, the decrease in pH would protonate a population of AnxA6 molecules, rendering them more hydrophobic and more prone to insertion into the MVs' bilayer (Veschi et al., 2020). The decrease in pH during apatite formation was reported (Smith et al., 2005; Tye et al., 2010; Blair et al., 2018), while the pH drop inside MVs has never been formally observed. Therefore, a first aim was to verify, using fluorescein as pH-sensitive probe (Sjöback et al., 1995), if the pH inside MVs effectively decreased during apatite formation. Thereafter, to determine the mechanism(s) of AnxA6 binding and its effect on membrane ordering (membrane fluidity), we used a fluorescent probe, 4-(14-phenyldibenzo[a,c]phenazin-9(14H)-yl)-phenol (DPAC) which was synthesized according to earlier reports (Dou et al., 2017; Zhang et al., 2020; Zhou et al., 2016). The fluorescent probe was mixed with liposomes as MV membrane model. DPAC has typical Vibration-Induced-Emission (VIE) properties (Zhang et al., 2020) due to changes in configuration and bent-to-planar motion depending on the restriction of molecular vibrations (Figure 1).

We hypothesized that the restriction of molecular vibration occurs when changing the environment of the probe, such as during transition from liquid to gel phase in the lipid bilayer induced by interaction of AnxA6 with the membrane. Therefore, DPAC was used to follow AnxA6 effect on the MV-mimicking vesicles and sense fluidity variations in membranes depending on the pH of the buffer. Our findings shed light into AnxA6 mechanism(s) of binding to MVs. They indicate for the first time that pH actually drops inside the MVs' lumen during apatite formation and highly suggest that this pH drop is responsible for AnxA6 translocation from the surface of the internal leaflet to the external phospholipid bilayer of the MVs.

2 | EXPERIMENTAL SECTION

2.1 | Material

Tris, citrate, EGTA, dimyristoylphosphatidylcholine (DMPC), dipalmitoylphosphatidylserine (DPPS), fluorescein were purchased from Sigma (Saint Quentin Fallavier, France). They were of the highest purity available.

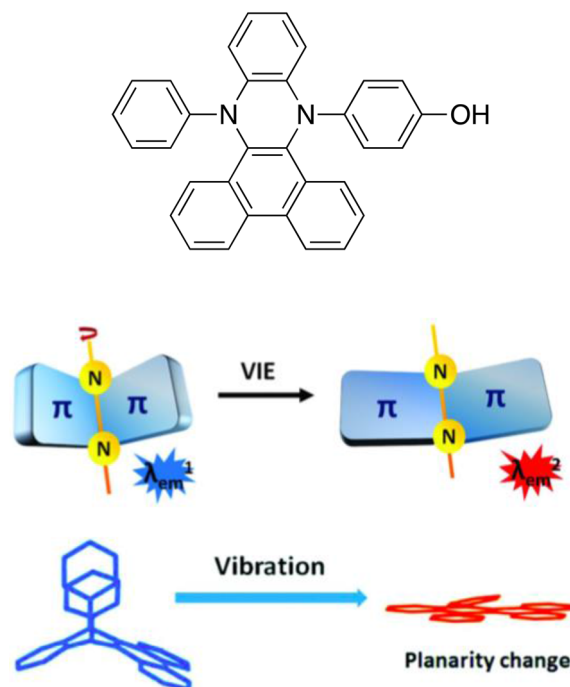


FIGURE 1 Mechanism of emission colour shift of DPAC upon VIE (Dou et al., 2017). Planarity changes in DPAC orientation induce a shift in the fluorescence emission toward the red edge when probe orientation is planar

4-(14-phenyldibenzo[a,c]phenazin-9(14H)-yl)-phenol (DPAC) was prepared according to (Zhou et al., 2016). Water was purified with a Milli-Q system, its resistivity was greater than 18 M Ω . Recombinant human AnxA6 protein was expressed and purified as described previously (Kirilenko et al., 2002).

2.2 | Purification of matrix vesicles

MVs were isolated from growth plates and epiphyseal cartilage slices of 17-day-old chicken embryos by collagenase digestion (Buchet et al., 2013). Leg bones from 17-day-old chicken embryos were cut into 1–3-mm thick slices and washed five times in a synthetic cartilage lymph (SCL) containing 100 mM NaCl, 12.7 mM KCl, 0.57 mM MgCl₂, 1.83 mM NaHCO₃, 0.57 mM Na₂SO₄, 1.42 mM NaH₂PO₄, 5.55 mM D-glucose, 63.5 mM sucrose and 16.5 mM 2-[[1,3-dihydroxy-2-(hydroxymethyl)propan-2-yl]amino]ethanesulfonic acid (TES) at pH 6.5. SCL was weakly buffered by phosphate and carbonate so that pH variation can be determined. Growth plate and epiphyseal cartilage slices were digested at 37°C for 3.5 h in the SCL buffer with 1 mM Ca²⁺ and collagenase (200 U of collagenase type 1A/g of tissue). It was vortexed and filtered through a nylon membrane. The suspension was centrifuged at 600 \times g for 10 min to pellet hypertrophic chondrocytes. The supernatant was centrifuged at 13,000 \times g for 20 min. The pellet was discarded and the supernatant was submitted to a third centrifugation at 70,000 \times g for 1 h. The supernatant was discarded and the final pellet containing MVs was washed several times and suspended in 500 μ l of SCL buffer and stored at 4°C. The protein concentration in the MV fraction was determined using the Bradford assay.

2.3 | Monitoring pH variation in matrix vesicles during mineralization

An aliquot of 500 μ l SCL medium containing MVs (see above) was completed with 2 mM total Ca²⁺ and 3.4 mM total phosphate and mineralization allowed to proceed at 37°C after 0, 2 h, 24 h and 168 h incubation. The external pH was monitored by incubating intact MVs with 0.1 μ M fluorescein. To determine internal pH, MV membrane bilayers were broken by six freeze-thaw cycles (5 min in liquid nitrogen, 10 min at 37°C) to release the internal protons in MVs into the extracellular medium. In both cases, the pH was monitored by measuring fluorescence emission intensity at 515 nm with a fixed excitation wavelength of 488 nm with 0.1 μ M fluorescein as pH indicator.

The internal concentration of free H^+ (C_{int}) was estimated by using Equation (2) which allowed an approximate determination of the internal apparent pH in MVs.

$$(C_{int} \times V_{int}) + (C_{ext} \times V_{ext}) = (C_{tot} \times V_{tot}) \quad (2)$$

Where the internal volume (V_{int}) of MVs was estimated to be around 11 μl over 500 μl total SCL volume (V_{tot}) with a protein concentration of 1 mg ml^{-1} , protein to lipid ratio of 1 mg:3 mg, bilayer density of 1.4 and MV diameter of 200 nm. The external volume corresponded to 489 μl (V_{ext}). The concentration of H^+ in the extracellular medium was determined (before freeze-thaw (C_{ext})), while the total concentration of H^+ was determined after freeze-thaw (external + internal medium, C_{tot}).

2.4 | Liposome preparation with embedded fluorescent probe

Liposomes were prepared by using the thin film hydration method (MacDonald et al., 1991; Mayer et al., 1986). Briefly, lipids composed of DMPC or DMPC-DPPS (9:1 mol:mol) in 1 ml chloroform (a total lipid mass of 2 mg) were mixed in a round flask, and fluorescent probe was added at 0.2 μM final concentration while heating above the lipid melting point. The solvent was dried under vacuum at 40°C on a rotatory evaporator to form a lipid film on the glass surface. The lipid film was hydrated in 1 ml of either 50 mM Tris-HCl buffer, pH 7.4 or 50 mM Citrate buffer, pH 5.4. This resulted in the formation of Multilamellar Vesicles (MLVs) with various sizes and numbers of layers. Six freeze-thaw cycles in liquid nitrogen and at 37°C in a water bath were then applied to obtain Large Unilamellar Vesicles (LUVs). The size of these LUVs was defined by extrusion through a porous membrane with a Mini-Extruder (Avanti Polar Lipids, Alabaster, AL, USA). The liposomes were heated above their phase-transition temperature (T_m), extruded through a 400 nm and then a 200 nm pore diameter polycarbonate membrane using a MiniExtruder apparatus (Avanti). The size of the liposome particles was rather homogeneous and around 240 nm, as measured with dynamic light scattering (DLS). The final liposome solution was stored at 4°C.

2.5 | Preparation of proteoliposomes and monitoring of the membrane physical state

To simulate MVs in a biomimetic environment, 0.08 mM DMPC or DMPC-DPPS (9:1 mol:mol) liposomes, mimicking the external and internal leaflet of MVs, respectively, were incubated with 1 μM AnxA6, and 2 mM Ca^{2+} , in either 50 mM Tris-HCl buffer, pH 7.4 or 50 mM Citrate buffer, pH 5.4. After 20 h of incubation at 37°C, gently shaking the samples, fluorescence emission spectra were measured (at 37°C) with an excitation wavelength fixed at 340 nm (based on absorption properties of DPAC). Since DPAC emission wavelength changes with membrane fluidity, the measurement of the Generalized Polarization (GP) parameter was appropriate to quantify membrane fluidity. The GP is related to probe-surrounding solvent mobility (Parasassi et al., 1990) and is calculated from fluorescence emission intensities according to the following Equation (3):

$$GP = I_{gel} - I_{LC} / (I_{gel} + I_{LC}) \quad (3)$$

where I_{gel} and I_{LC} are, respectively, intensity values of the probe to characteristic emission wavelengths of gel or liquid-crystal phases. In this context, I_{gel} was determined at 450 nm and I_{LC} was measured at 560 nm.

2.6 | Helsinki statement

CNRS, University of Lyon, and Nencki Institute of Experimental Biology in Warsaw, Poland are committed to the 3Rs (replacement, refinement and reduction of animals in research) and have an ethical review procedure for licensed animal use. It was considered good practice to build on the existing knowledge and expertise to extend this to nonlicensed animal and tissue use. The use of chick embryos was considered as nonlicensed animal use and full animal ethics committee approval was not required for this use.

3 | RESULTS

3.1 | Calibration of fluorescein for the determination of pH

A pH drop is expected to occur within MVs during apatite formation (Blair et al., 2018), due to the release of protons in the reaction (1), yet this decrease has never been experimentally demonstrated. Therefore, fluorescein (Figure 2a) was used as a pH

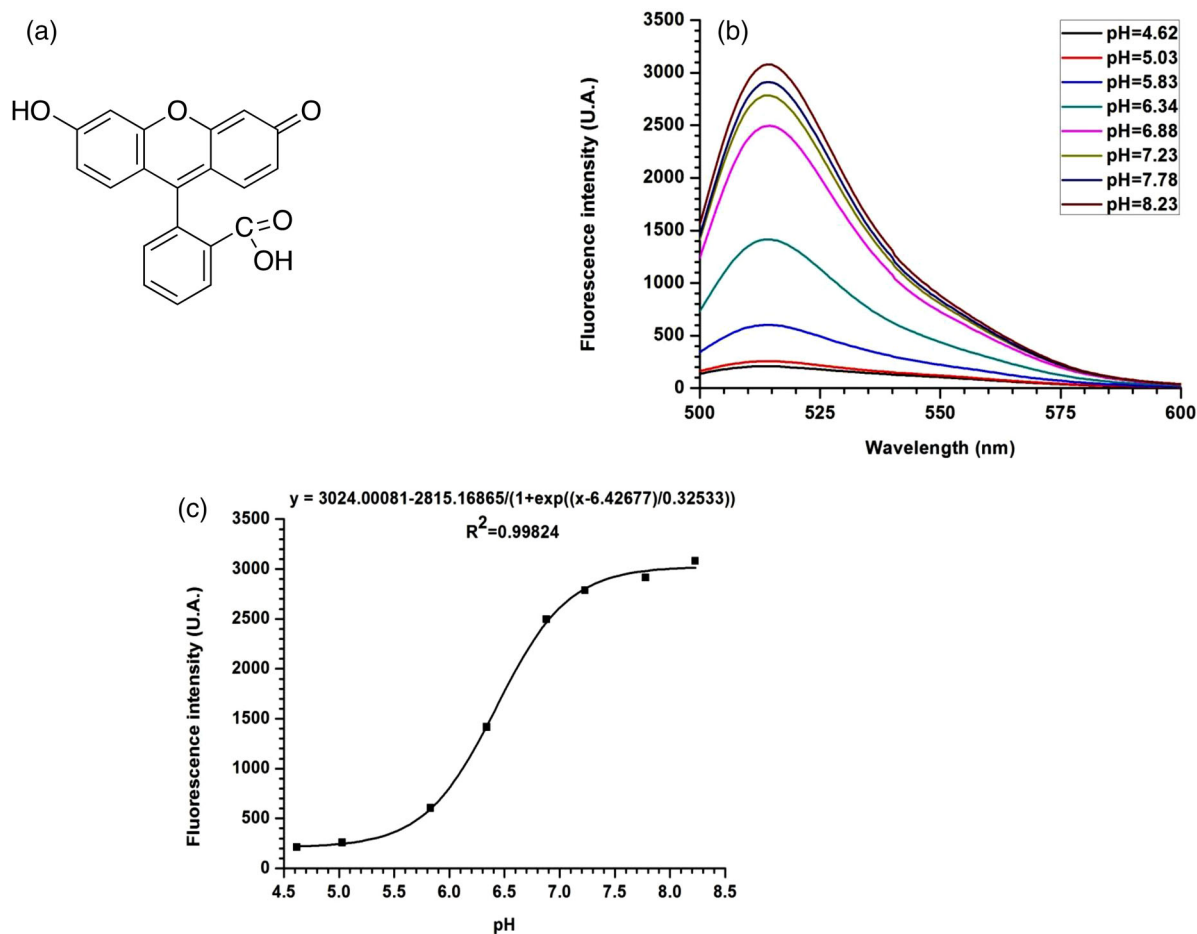


FIGURE 2 (a). Chemical structure of fluorescein. (b). Typical fluorescence spectra of fluorescein ($0.1 \mu\text{M}$, λ_{ex} 488 nm) recorded in 10 mM phosphate solution adjusted to pH 5.0; 5.8; 6.4; 6.9 and 7.2 in the presence of 2 mM Ca^{2+} at 37°C. (c). Fluorescence intensity measured at 515 nm as a function of pH. Full line, sigmoidal fit obtained for experimental data

sensor to measure the pH of the solution during apatite formation. Firstly, fluorescence emission spectra of fluorescein were recorded at various pH values. The fluorescence intensity strongly depended on pH, with a pronounced intensity decrease when the pH of the buffer decreased from 7.2 to 5.0 (Figure 2b). A sigmoid variation of the fluorescence intensity measured at 515 nm (using a 488 nm excitation wavelength) within this pH range allowed us to plot a calibration curve (Figure 2c). A pKa around 6.4 was determined for fluorescein, in good agreement with the literature (Sjöback et al., 1995), which makes it a convenient pH sensor within the pH range expected to occur in MVs during mineralization

3.2 | The internal pH of matrix vesicles decreased during mineralization

To simulate mineralization, 2 mM calcium and 3.4 mM phosphate ions (final concentrations) were added to MVs in SCL together with $0.1 \mu\text{M}$ fluorescein. At the selected incubation time points of 0 h, 2h, 24h, and 1 week (168h), the pH of the sample was determined before and after six freeze/thaw cycles to induce MV burst and release of the intraluminal content. We observed a continuous and significant decrease in pH from 6.3 to 5.8 during the first 24 h in the case of MVs subjected to six freeze/thaw cycles (Figure 3a). On the contrary, the pH before burst (Figure 3b) remained rather stable, confirming that the decrease in the pH previously observed after MV burst can be explained by a strong drop in the pH inside MVs as the apatite formation progressed. After 1-week incubation, the pH dropped drastically to 5.1. The same pH values were measured inside and outside MVs (before and after burst), indicating that the vesicles were already broken, even without any freeze/thaw cycle. This was probably caused by apatite crystal formation disrupting the MV membrane and releasing protons (Equation 1) into the medium.

The significant decrease of the pH in the bulk solution after MV burst (from 6.3 to 5.8, $p < 0.001$, during the first 2h) corresponded to an estimated decrease in the pH inside MVs from 6.3 to 5.6. This decrease was more pronounced after

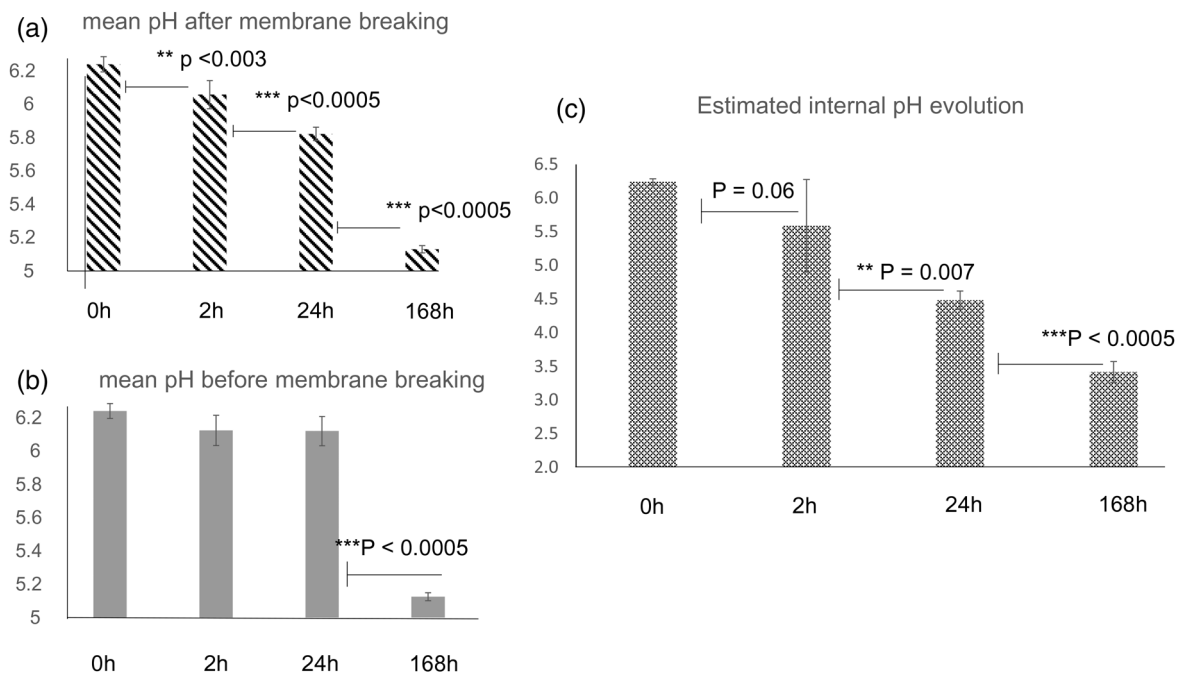


FIGURE 3 Mean pH values of MVs in SCL buffer containing 3.4 mM phosphate either after (a) or before (b) membrane breaking, as determined by fluorescein, measured at different times ($t = 0\text{h}$, 2h , 24h , 1 week) after adding 2 mM calcium ions. Estimated internal pH (c), according to Equation (2). Plot of representative means ($\pm\text{SD}$) of five independent experiments. p obtained with Student t -test

24 h-incubation, when the pH dropped from 6.3 to 4.5. After 1 week incubation, MVs were broken in association with maximal internal pH of 3.4 (Figure 3c).

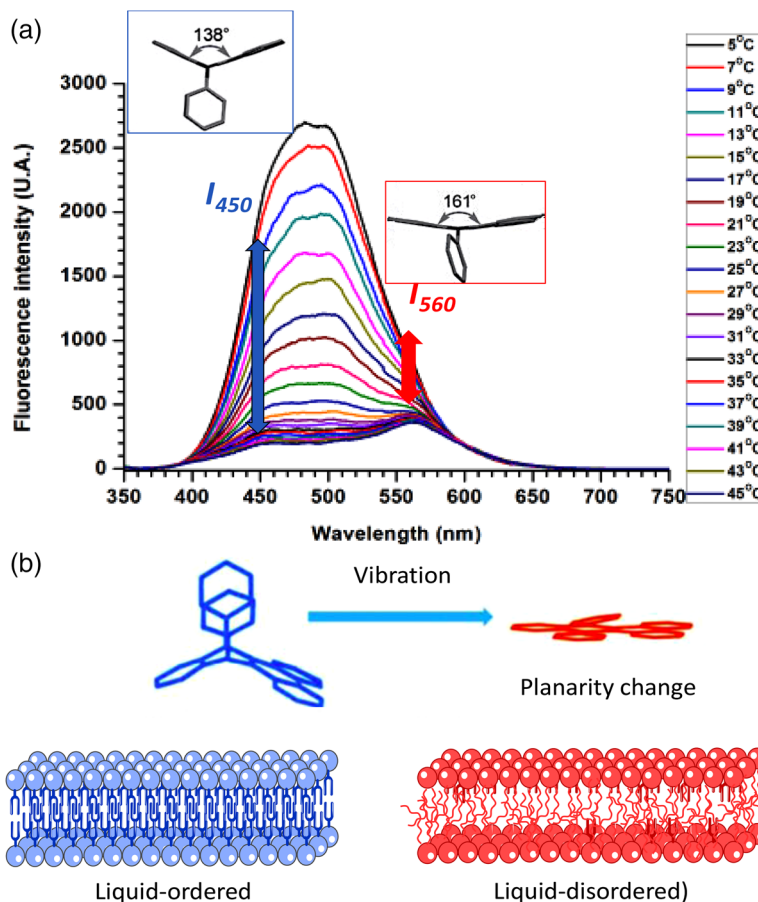
This pH decrease following apatite formation within MVs can have profound consequences on proteins present in the MVs' lumen and notably on the highly abundant AnxA6. AnxA6 is thought to translocate over the MV membrane with an intermediary transmembrane state (Veschi et al., 2020). AnxA6 has an isoelectric point (pI) around 5, therefore the above-mentioned pH drop would change AnxA6's ionization state, increase its surface hydrophobicity aiding protein insertion into the bilayer (Golczak et al., 2001; Veschi et al., 2020). Such insertion would not be without consequences on membrane organization. Liposome or even membrane cell binding of Anx6 were shown to induce membrane remodelling (Alvarez-Guaita et al., 2015; Cornely et al., 2011; Enrich et al., 2011).

3.3 | Validation of 4-(14-phenyldibenzo[a,c]phenazin-9(14H)-yl)-phenol probe as a sensor of membrane order

Anx6-membrane interactions under different pHs were monitored with a home-made fluorescent probe, DPAC, which undergoes spectral changes caused by transformation from bent to planar form. Such transformation, resulting from restriction of molecular vibrations, may occur when Anx6 binds to the membrane and may differ according to the interaction mode. Generally, when a protein binds to the membrane surface, a decrease in the membrane fluidity is observed due to the removal of water molecules in the vicinity of head polar groups of phospholipids (Francois-Moutal et al., 2016; Francois-Moutal et al., 2013; Francois-Moutal et al., 2014). On the contrary, protein insertion into the membrane bilayer increases membrane fluidity as the lipid head groups are thread apart, which yields an overall mobility of the bilayer (Francois-Moutal et al., 2013). DPAC was used to determine the type of AnxA6 binding onto the membrane under two pH conditions: $\text{pH} = 5.4$ (50 mM citrate buffer) and $\text{pH} = 7.4$ (50 mM Tris-HCl buffer). We used liposomes containing either DMPC to mimic the outer leaflet of the MVs' membrane or a DMPC:DPPS (9:1) mixture to mimic the inner leaflet. To validate DPAC as a fluorescent probe on the membrane fluidity, we recorded its fluorescence emission spectra in either DMPC or DMPC-DPPS (9:1) liposomes at $\text{pH} 7.4$ or $\text{pH} 5.4$, between 400 and 700 nm using a 340 nm excitation wavelength at temperature range from 5°C to 45°C . For example, DPAC inserted in DMPC-DPPS (9:1) membranes shows a large Stokes-shifted emission with two emission peaks at 450 and 560 nm (Figure 4a) typical from VIE properties. From lower to higher temperature, the blue emission wavelength ($\lambda_{\text{em}} = 450\text{ nm}$) extensively decreased while the red emission ($\lambda_{\text{em}} = 560\text{ nm}$) slightly increased (Figure 4a).

DPAC presents a folded state with a blue emission in a membrane gel-like state at low temperature, while it presents a stretched state with a red fluorescence emission in a nonrestricted environment, as in a membrane fluid-like state, as described by Wang

FIGURE 4 (a). Fluorescence emission spectra (λ_{ex} 340 nm) of DPAC in DMPC:DPPS (9:1) liposomes in citrate buffer (50 mM, pH 5.4) from 5°C to 45°C. (b). Scheme of DPAC inserted in rigid or fluid membranes. The planar configuration can be solely adopted in fluid phases, where molecular vibrations are not restricted



et al. (2018). As a consequence, molecular vibrations of DPAC at low temperature, were microcosmically restricted with higher steric hindrance and significant nonplanar distortions (i.e., a saddle shape) (Figure 4b). Therefore, our results indicate that DPAC is a good sensor of the fluidity state (gel/ordered to liquid/disordered) of the membrane. Such temperature-dependency of the emission peak wavelength, is reminiscent of Laurdan properties (Parasassi et al., 1991), a well known fluorescent molecule widely used to sense membrane physical state variation upon lipid-ligand interaction (Bagatolli, 2012). By analogy with the Laurdan, a GP parameter (Equation 3) was calculated from the emission wavelength of DPAC inserted in liposomes. The fluorescence emission intensities at 450 nm (ordered/gel-phase like marker) and 560 nm (disordered/ liquid-like phase marker) were selected to determine the relative amount of gel and liquid phases when they coexist in liposomes. For all liposomes tested (DMPC and DMPC:DMPS (9:1)), both in citrate (pH 5.4) and Tris HCl (pH 7.4) buffers, GP declined with the increase in temperature (Figure 5). In all cases, lipid membrane turned out to be more fluid and liquid-disordered with increasing temperature. Its decrease was more pronounced in DMPC proteoliposomes at acid pH as compared to DMPC proteoliposomes in neutral state. These findings confirm that GP is valid for DPAC and that this fluorescent probe may sense changes in the liposome fluidity during AnxA6 binding.

3.4 | Determination of the types of AnxA6 interactions with membrane bilayers caused by the acidification as monitored by the membrane fluidity changes

The proteoliposomes were enriched in AnxA6 to determine the nature of the interactions of AnxA6 with membrane bilayers during acidification from pH 7 (Tris HCl buffer) to pH 5.4 (citrate buffer). Fluorescence spectra of DPAC were recorded at 37°C before and 2h after addition of 1 μM AnxA6 to liposomes, in the presence of 2 mM calcium. Fluorescence intensities were measured at 450 nm (ordered phase) and 560 nm (disordered phase) and GP values were calculated for each sample as described above. ΔGP was calculated from GP values obtained before and after incubation with AnxA6 ($\Delta\text{GP} = \text{GP}_{\text{liposome+AnxA6}} - \text{GP}_{\text{liposome}}$) to illustrate the fluidity changes upon protein binding (Figure 6).

Addition of AnxA6 to DMPC at pH 7.4 or at pH 5.4 or addition of AnxA6 to DMPC-DPPS (9-1) at pH 7.4, resulted in a positive GP variation (ΔGP) (Figure 6) indicating that AnxA6 induced a decrease in the mobility of solvent molecules in the vicinity of DPAC. This suggested an increase of the rigidity of the membrane and was consistent with AnxA6 bound to the

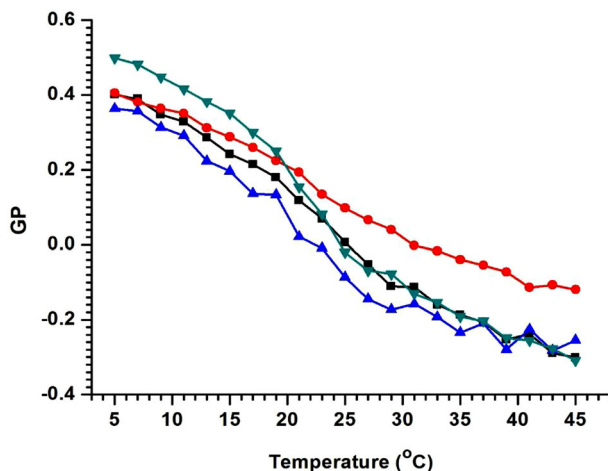


FIGURE 5 GP of DPAC in membrane bilayers of liposome as a function of temperature from 5°C to 45°C. Liposomes were composed by: DMPC in Tris HCl buffer, pH 7.4 (Green triangles), DMPC in citrate buffer, pH 5.4 (Blue triangles), DMPC-DPPS (9:1) in Tris HCl buffer, pH 7.4 (Red circles) and DMPC-DPPS (9:1) in citrate buffer, pH 5.4 (Black squares)

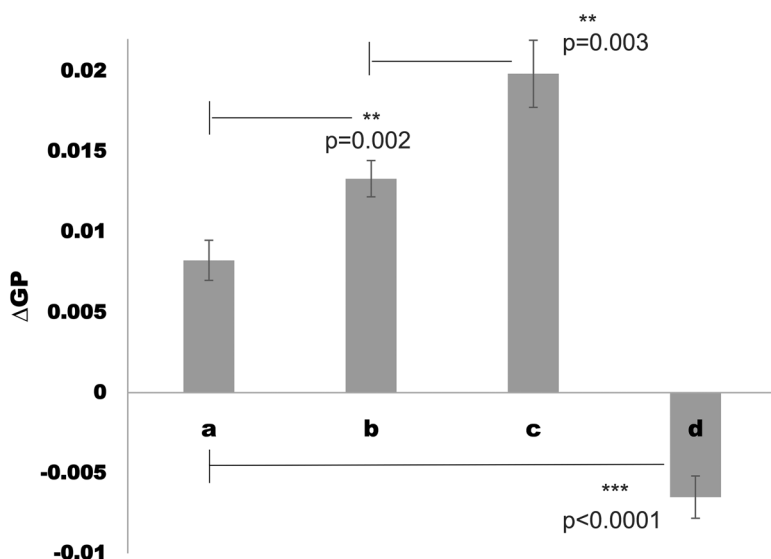


FIGURE 6 ΔGP values ($GP_{\text{liposome+AnxA6}} - GP_{\text{liposome}}$) of DPAC in liposomes after AnxA6 binding. (a) DMPC in Tris HCl buffer pH7.4; (b) DMPC:DPPS (9:1) in Tris HCl buffer pH 7.4; (c) DMPC in citrate buffer pH = 5.4; (d) DMPC: DPPS (9:1) in Citrate buffer pH 5.4 obtained at 37°C after 2 h of AnxA6 incubation. Measurements were done from five independent samples

surface of membrane bilayer. AnxA6 binding on the surface of the bilayer, displaced water molecules from the surface of the membrane, which resulted in the formation of more rigid membrane bilayer as schematically depicted in Figure 7.

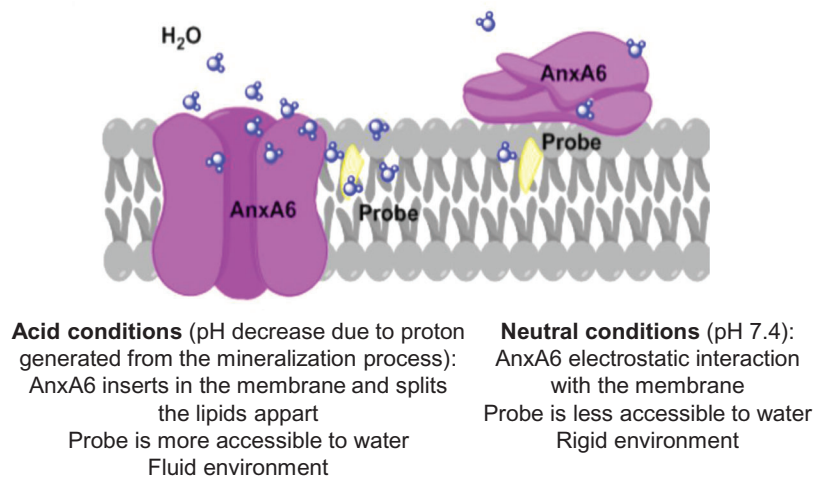
In contrast, the addition of AnxA6 to DMPC-DPPS (9:1) at pH 5.4 induced a negative ΔGP , suggesting that a distinct type of AnxA6 interaction with anionic phospholipids occurred at pH 5.4 as compared with that with neutral phospholipids. This was interpreted as AnxA6 increased the mobility of solvent molecules in the vicinity of DPAC. Due to the bulky 3D structure of protein, its membrane insertion would expand the gap between lipids and DPAC would have more access to water (Figure 7). From these findings, we infer that under acidic conditions and only in the presence of ionic phospholipids, AnxA6 inserted into bilayer membrane or evoked membrane bilayer splitting apart the phospholipids.

4 | DISCUSSION

4.1 | Apatite formation induced a decrease in pH inside MVs

The formation of apatite occurred in the MVs' lumen, and not on the external surface of MVs, since the internal pH dropped from 6.25 to 4.48 inside MVs after 24h incubation, while the external pH remained constant after 24h incubation. This confirms previous reports that apatite nucleation is initiated inside MVs and not on its external surface (Anderson, 2003; Bottini et al.,

FIGURE 7 Location of AnxA6 at the DMPC-DPPS bilayer under acidic (left) and neutral (right) conditions



2018; Golub, 2009; Plaut et al., 2019; Wuthier et al., 2011). The starting pH of 6.25 is also close to the pH optimum of 6.7 for PHOSPHO1 activity (Roberts et al., 2004) the enzyme that has been implicated in the intravesicular production of Pi for initiation of apatite formation in the MVs' lumen (Roberts et al., 2007). Assuming an average of eight protons which are released per apatite (Equation 1) and taking into account that about one mol of carbonate per mol of apatite was present, the pH values corresponded to 1.5 % of the total calcium used to form apatite inside MVs after 24 h, while not more than 0.25 % of the total concentration was employed outside MVs. After 168 h, MVs were broken probably due to mechanic forces caused by the accumulation of calcium phosphate minerals (Plaut et al., 2019) and/or lipase activity (Stechschulte et al., 1992). After 168 h, 27 % of total calcium concentration was used to form apatite. Only a fraction of calcium ions was taken due to the acidic environment, which could prevent continuous apatite formation.

The amount of calcium amassed in apatite could be underestimated since to sustain mineral formation, MVs probably responded to the acid stress with bicarbonate ions to neutralize the excess hydrogen ions ($H^+HCO_3^-H_2O + CO_2$) catalysed by carbonic anhydrase II, which is present in MVs (Marsh, 2008).

4.2 | Distinct types of lipid interactions support a possible translocation mechanism of AnxA6 from the lumen into the membrane bilayer

AnxA6 is located in the lumen of MVs, on the inner leaflet of MVs, inside the lipid bilayer of MVs and on the outer leaflet of MVs (Veschi et al., 2020). Here we provided experimental evidence that apatite formation induced acidification inside MVs. The membrane fluidity increased in the case of AnxA6 interaction with DMPC-DPPS (9:1) during acidification as compared to that of DMPC-DMPS (9:1) without AnxA6. This was in contrast to the AnxA6 interaction with DMPC-DMPS (9:1) under neutral conditions, where the membranes became more rigid. It indicated unambiguously that AnxA6 interacted in a distinct manner with DMPC-DMPS (9:1) at pH 5.4 and then at pH 7.4. We concur that acidification may trigger the translocation of AnxA6 inside the bilayer by increasing the hydrophobicity of AnxA6, as it has been earlier proposed (Golczak et al., 2001; Veschi et al., 2020). It is established that proteins or peptides corresponding to hydrophobic putative transmembrane channel segments are capable of self assembly in lipid bilayers (Marsh, 2008). The origin of the driving force of insertion is that transmembrane sequences appear to have a markedly nonpolar character. Although spontaneous protein insertion from the cytoplasmic side into bilayer upon acidification is rarely reported, it was earlier recognized that AnxA6 can interact on the surface of phosphatidylserine (Alvarez-Guaita et al., 2015; Bandorowicz & Pikuła, 1993; Enrich et al., 2011; Gerke & Moss, 2002; Veschi et al., 2020) (mimicking the inner leaflet), as well as on the surface of phosphatidylcholine (Alvarez-Guaita et al., 2015; Veschi et al., 2020) (mimicking the outer leaflet) and can accidentally form transmembrane ion channels (Golczak et al., 2001; Kirsch et al., 2000). Calcium influx coupled to the interaction of AnxA6 with S100A8 and S100A9 proteins may facilitate translocation of AnxA6 from the inner to the outer leaflet of the plasma membrane (Bode et al., 2008; Grewal et al., 2017). The translocation mechanism during acidification appeared to be unidirectional, that is from the MVs' lumen toward the extracellular side of MVs. This was inferred from the observed property of proteoliposomes enriched with DMPC and AnxA6, when during acidification, the proteoliposomes become more rigid. This finding was interpreted as AnxA6 interacting on the surface of the DMPC bilayer and not penetrating inside the bilayer. In this context, DMPC mimics the external side of the MV bilayer.

4.3 | Functions of AnxA6 and physiological relevance

AnxA5 and AnxA6 may not represent the essential annexins that promote mineralization *in vivo* (Belluoccio et al., 2010; Belluoccio et al., 2010). The development of skeletal elements was not significantly impaired by the absence of annexins (Brachvogel et al., 2003; Grskovic et al., 2012). Depletion of AnxA5, AnxA6 and collagen type X caused no changes in MV-mediated mineralization (Grskovic et al., 2012). However, primary chondrocyte cultures isolated from rib cartilage of newborn AnxA6^{-/-} mice showed delayed terminal differentiation as indicated by reduced terminal differentiation markers, including tissue-nonspecific alkaline phosphatase (TNAP), matrix metalloproteinase-13, osteocalcin and Runx2, and reduced mineralization (Minashima et al., 2012). Absence of AnxA6 can be compensated by other members of the annexin family (Enrich et al., 2017), while under stress conditions, such as partial hepatectomy, AnxA6 could be essential for survival (Alvarez-Guaita et al., 2020). Distinct types of interactions between lipids and AnxA6 in MVs could reflect distinct functions (Veschi et al., 2020). Besides its ability to recruit proteins, cholesterol, and to reorganize lipid raft domains (Cornely et al., 2011), AnxA6 on the inner side of MVs may form a nucleation core enriched with calcium ions and phosphatidylserine to facilitate the initiation of apatite inside MVs, similarly to the nucleation core formed by AnxA5, phosphatidylserine and calcium ions (Genge et al., 2007). Finally, AnxA6 on the outer side of MVs (Kirsch et al., 2000), as AnxA5 (Bolean et al., 2017; Bolean et al., 2020) may bind to collagen to facilitate the binding of MVs to collagen fibres to propagate mineral depositions in ECM. However, there are still no experimental evidence that AnxA6 interacts with collagen fibres.

5 | CONCLUSION

Our findings indicated that apatite formation was initiated in the lumen of MVs and induced a decrease in the intravesicular pH. We propose a mechanism of unidirectional AnxA6 translocation from the inner leaflet of the MVs' bilayer, into the MV bilayer, toward the external surface of MVs. This interpretation is supported by the fluidity property of proteoliposomes containing AnxA6 and enriched with either DMPC, modelling the outer leaflet of MVs, or DMPC:DMPS (9:1) corresponding to the inner leaflet of MVs. Upon acidification, AnxA6 became hydrophobic, facilitating its insertion in DMPC:DMPS (9:1) as revealed by the increased fluidity compared to the interaction with pure DMPC membranes. These results are in accordance with the differential scanning calorimetry (DSC), atomic force microscopy (AFM) and circular dichroism (CD) data previously published by Buzhynskyy et al. (2009) and Veschi et al. (2020). Those data refer to the possible mechanism of AnxA6 insertion into the membrane bilayer and reinforce the synergy of AnxA6, PS, Ca²⁺ associated with pH changes in the fine adjustment of apatite nucleation process.

ACKNOWLEDGEMENTS

The authors thank the University Claude Bernard Lyon1, CNRS and the Auvergne-Rhone-Alpes Region (SCUSI 2017 009361 01) for financial support. This work was also supported by the projects: HC **Partnership Programs** POLONIUM 2018/2019 to A. Strzelecka-Kiliszek and L. Ben Trad, POLONIUM 2021/2022 to A. Strzelecka-Kiliszek and S. Mebarek from NAWA, an ERA-CVD/MICROEXPLORATION/4/2018 grant from the National Centre for Research and Development, Poland to S. Pikula; Opus grant 2016/23/B/NZ3/03116 from the National Science Centre to J. Bandorowicz-Pikula, the statutory funds of the Nencki Institute of Experimental Biology, Polish Academy of Sciences; Fundação de Amparo à Pesquisa do Estado de São Paulo (FAPESP, grants **2019/08568-2**; **2019/25054-2**), Coordenação de Aperfeiçoamento de Pessoal de Nível Superior (CAPES, Finance Code 001, 1738449, 88887.320304/2019-00,) and Conselho Nacional de Desenvolvimento Científico e Tecnológico (CNPq, 304021/2017-2) for the financial support given to our laboratory. We acknowledge the Brazil-France USP-COFECUB Uc Sv 184/20 grant. E. Amabile Veschi and Maytê Bolean received a CAPES scholarship. P. Ciancaglini and A.P. Ramos are CNPq researchers.

ORCID

Ofelia Maniti  <https://orcid.org/0000-0001-9371-9580>

Layth Ben Trad  <https://orcid.org/0000-0003-4770-9765>

Massimo Bottini  <https://orcid.org/0000-0001-9237-8972>

René Buchet  <https://orcid.org/0000-0002-7966-3856>

REFERENCES

- Alvarez-Guaita, A., Blanco-Muñoz, P., Meneses-Salas, E., Wahba, M., Pollock, A. H., Jose, J., Casado, M., Bosch, M., Artuch, R., Gaus, K., Lu, A., Pol, A., Tebar, F., Moss, S. E., Grewal, T., Enrich, C., & Rentero, C. (2020). Annexin A6 is critical to maintain glucose homeostasis and survival during liver regeneration in mice. *Hepatology*, 72, 2149–2164, <https://doi.org/10.1002/HEP.31232>
- Alvarez-Guaita, A., Vilà de Muga, S., Owen, D. M., Williamson, D., Magenau, A., García-Melero, A., Reverter, M., Hoque, M., Cairns, R., Cornely, R., Tebar, F., Grewal, T., Gaus, K., Ayala-Sanmartín, J., Enrich, C., & Rentero, C. (2015). Evidence for annexin A6-dependent plasma membrane remodelling of lipid domains. *British Journal of Pharmacology*, 172, 1677–1690, <https://doi.org/10.1111/BPH.13022>

- Anderson, H. C. (2003). Matrix vesicles and calcification. *Current Rheumatology Reports*, 5, 222–226. <https://doi.org/10.1007/s11926-003-0071-z>
- Aoba, T., & Moreno, E. C. (1992). Changes in the solubility of enamel mineral at various stages of porcine amelogenesis. *Calcified Tissue International*, 50, 266–272. <https://doi.org/10.1007/BF00296292>
- Bagatolli, L. A. L. A. U. R. D. AN. F. Fluorescence Properties in (2012). Membranes: A journey from the fluorometer to the microscope., 3–35. https://doi.org/10.1007/4243_2012_42
- Bandorowicz, J., & Pikuła, S. (1993). Annexins—multifunctional, calcium-dependent, phospholipid-binding proteins. *Acta Biochimica Polonica*, 40, 281–293.
- Bandorowicz-Pikuła, J., & Pikuła, S. (1998). Annexins and ATP in membrane traffic: A comparison with membrane fusion machinery. *Acta Biochimica Polonica*, 45, 721–733.
- Belluoccio, D., Etich, J., Rosenbaum, S., Frie, C., Grskovic, I., Stermann, J., Ehlen, H., Vogel, S., Zaucke, F., von der Mark, K., Bateman, J. F., & Brachvogel, B. (2010). Sorting of growth plate chondrocytes allows the isolation and characterization of cells of a defined differentiation status. *Journal of Bone and Mineral Research*, 25, 1267–1281. <https://doi.org/10.1002/JBMR.30>
- Belluoccio, D., Grskovic, I., Niehoff, A., Schlötzer-Schrehardt, U., Rosenbaum, S., Etich, J., Frie, C., Pausch, F., Moss, S. E., Pöschl, E., Bateman, J. F., & Brachvogel, B. (2010). Deficiency of annexins A5 and A6 induces complex changes in the transcriptome of growth plate cartilage but does not inhibit the induction of mineralization. *Journal of Bone and Mineral Research*, 25, 141–153. <https://doi.org/10.1359/JBMR.090710>
- Berendsen, A. D., & Olsen, B. R. (2015). Bone development. *Bone (New York)*, 80, 14–18. <https://doi.org/10.1016/j.bone.2015.04.035>
- Blair, H. C., Larrouture, Q. C., Tourkova, I. L., Liu, L., Bian, J. H., Stolz, D. B., Nelson, D. J., & Schlesinger, P. H. (2018). Support of bone mineral deposition by regulation of pH. *American Journal of Physiology. Cell physiology*, 315, C587–C597. <https://doi.org/10.1152/AJPCELL.000562018/ASSET/IMAGES/LARGE/ZH00091883220006.JPEG>
- Blair, H. C., Zaidi, M., & Schlesinger, P. H. (2002). Mechanisms balancing skeletal matrix synthesis and degradation. *Biochemical Journal*, 364, 329–341. <https://doi.org/10.1042/bj20020165>
- Bode, G., Lüken, A., Kerckhoff, C., Roth, J., Ludwig, S., & Nacken, W. (2008). Interaction between S100A8/A9 and annexin A6 is involved in the calcium-induced cell surface exposition of S100A8/A9. *Journal of Biological Chemistry*, 283, 31776–31784. <https://doi.org/10.1074/JBC.M803908200>
- Bolean, M., Borin, I. A., Simão, A. M. S., Bottini, M., Bagatolli, L. A., Hoylaerts, M. F., Millán, J. L., & Ciancaglini, P. (2017). Topographic analysis by atomic force microscopy of proteoliposomes matrix vesicle mimetics harboring TNAP and AnxA5. *Biochimica et Biophysica Acta (BBA) - Biomembranes*, 1859, 1911–1920. <https://doi.org/10.1016/j.bbamem.2017.05.010>
- Bolean, M., Izzi, B., van kerckhoven, S., Bottini, M., Ramos, A. P., Millán, J. L., Hoylaerts, M. F., & Ciancaglini, P. (2020). Matrix vesicle biomimetics harboring Annexin A5 and alkaline phosphatase bind to the native collagen matrix produced by mineralizing vascular smooth muscle cells. *Biochimica et Biophysica Acta (BBA) - General Subjects*, 1864, 129629. <https://doi.org/10.1016/j.bbagen.2020.129629>
- Boskey, A. L., Bullough, P. G., & Posner, A. S. (1982). Calcium-acidic phospholipid-phosphate complexes in diseased and normal human bone. *Metabolic Bone Disease & Related Research*, 4, 151–156. [https://doi.org/10.1016/0221-8747\(82\)90029-7](https://doi.org/10.1016/0221-8747(82)90029-7)
- Bottini, M., Mebarek, S., Anderson, K. L., Strzelecka-Kiliszek, A., Zozycki, L., Simão, A. M. S., Bolean, M., Ciancaglini, P., Pikuła, J. B., Pikuła, S., Magne, D., Volkman, N., Hanein, D., Millán, J. L., & Buchet, R. (2018). Matrix vesicles from chondrocytes and osteoblasts: Their biogenesis, properties, functions and biomimetic models. *Biochimica et Biophysica Acta. General Subjects*, 1862, 532–546. <https://doi.org/10.1016/j.bbagen.2017.11.005>
- Brachvogel, B., Dikschas, J., Moch, H., Welzel, H., von der Mark, K., Hofmann, C., & Pöschl, E. (2003). Annexin A5 is not essential for skeletal development. *Molecular and Cellular Biology*, 23, 2907–2913. <https://doi.org/10.1128/MCB.23.8.2907-2913.2003>
- Buchet, R., Pikuła, S., Magne, D., & Mebarek, S. (2013). Isolation and characteristics of matrix vesicles. *Methods in Molecular Biology*, 1053, 115–124. https://doi.org/10.1007/978-1-62703-562-0_7
- Buzhynskyy, N., Golczak, M., Lai-Kee-Him, J., Lambert, O., Tessier, B., Gounou, C., Bérat, R., Simon, A., Granier, T., Chevalier, J. M., Mazères, S., Bandorowicz-Pikuła, J., Pikuła, S., & Brisson, A. R. (2009). Annexin-A6 presents two modes of association with phospholipid membranes. A combined QCM-D, AFM and cryo-TEM study. *J Struct Biol*, 168, 107–116. <https://doi.org/10.1016/j.jsb.2009.03.007> Epub 2009 Mar 21. PMID: 19306927
- Cornely, R., Rentero, C., Enrich, C., Grewal, T., & Gaus, K. (2011). Annexin A6 is an organizer of membrane microdomains to regulate receptor localization and signalling. *Iubmb Life*, 63, 1009–1017. <https://doi.org/10.1002/IUB.540>
- Dou, W. T., Chen, W., He, X. P., Su, J., & Tian, H. (2017). Vibration-Induced-Emission (VIE) for imaging amyloid β fibrils. *Faraday Discussions*, 196, 395–402. <https://doi.org/10.1039/C6FD00156D>
- Enrich, C., Rentero, C., de Muga, S. V., Reverter, M., Mulay, V., Wood, P., Koese, M., & Grewal, T. (2011). Annexin A6-Linking Ca(2+) signaling with cholesterol transport. *Biochimica et Biophysica Acta*, 1813, 935–947. <https://doi.org/10.1016/j.bbamcr.2010.09.015>
- Enrich, C., Rentero, C., & Grewal, T. (2017). Annexin A6 in the liver: From the endocytic compartment to cellular physiology. *Biochimica et Biophysica Acta (BBA) - Molecular Cell Research*, 1864, 933–946. <https://doi.org/10.1016/j.bbamcr.2016.10.017>
- Francois-Moutal, L., Maniti, O., Marcillat, O., & Granjon, T. (2013). New insights into lipid-Nucleoside Diphosphate Kinase-D interaction mechanism: Protein structural changes and membrane reorganisation. *Biochimica et Biophysica Acta (BBA) - Biomembranes*, 1828, 906–915. <https://doi.org/10.1016/j.bbamem.2012.08.023>
- Francois-Moutal, L., Marcillat, O., & Granjon, T. (2014). Structural comparison of highly similar nucleoside-diphosphate kinases: Molecular explanation of distinct membrane-binding behavior. *Biochimie*, 105, 110–118. <https://doi.org/10.1016/j.biochi.2014.06.025>
- Francois-Moutal, L., Ouberaï, M. M., Maniti, O., Welland, M. E., Strzelecka-Kiliszek, A., Wos, M., Pikuła, S., Bandorowicz-Pikuła, J., Marcillat, O., & Granjon, T. (2016). Two-step membrane binding of NDPK-B induces membrane fluidity decrease and changes in lipid lateral organization and protein cluster formation. *Langmuir*, 32, 12923–12933. <https://doi.org/10.1021/ACS.LANGMUIR.6B03789>
- Genge, B. R., Wu, L. N. Y., & Wuthier, R. E. (2007). In vitro modeling of matrix vesicle nucleation: Synergistic stimulation of mineral formation by annexin A5 and phosphatidylserine. *Journal of Biological Chemistry*, 282, 26035–26045. <https://doi.org/10.1074/JBC.M701057200>
- Gerke, V., & Moss, S. E. (2002). Annexins: From structure to function. *Mitochondrial Membrane Permeabilization in Cell Death*, 82, 331–371. <https://doi.org/10.1152/PHYSREV.00030.2001>
- Golczak, M., Kicinska, A., Bandorowicz-Pikuła, J., Buchet, R., Szewczyk, A., & Pikuła, S. (2001). Acidic pH-induced folding of annexin VI is a prerequisite for its insertion into lipid bilayers and formation of ion channels by the protein molecules. *Faseb Journal*, 15, 1083–1085. <https://doi.org/10.1096/FJ.00-0523FJE>
- Golub, E. E. (2009). Role of matrix vesicles in biomineralization. *Biochimica et Biophysica Acta (BBA) - General Subjects*, 1790, 1592–1598. <https://doi.org/10.1016/j.bbagen.2009.09.006>
- Grewal, T., Hoque, M., Conway, J. R. W., Reverter, M., Wahba, M., Beevi, S. S., Timpson, P., Enrich, C., & Rentero, C. (2017). Annexin A6-A multifunctional scaffold in cell motility. *Cell Adhesion & Migration*, 11, 288–304. <https://doi.org/10.1080/19336918.2016.1268318>
- Grskovic, I., Kutsch, A., Frie, C., Groma, G., Stermann, J., Schlötzer-Schrehardt, U., Niehoff, A., Moss, S. E., Rosenbaum, S., Pöschl, E., Chmielewski, M., Rappl, G., Abken, H., Bateman, J. F., Cheah, K. S., Paulsson, M., & Brachvogel, B. (2012). Depletion of annexin A5, annexin A6, and collagen X causes no gross changes

- in matrix vesicle-mediated mineralization, but lack of collagen X affects hematopoiesis and the Th1/Th2 response. *Journal of Bone and Mineral Research*, 27, 2399–2412, <https://doi.org/10.1002/JBMR.1682>
- Hallett, S. A., Ono, W., & Ono, N. (2019). Growth plate chondrocytes: Skeletal development, growth and beyond. *International Journal of Molecular Sciences*, 20, 10.3390/ijms20236009
- Kirilenko, A., Golczak, M., Pikula, S., Buchet, R., & Bandorowicz-Pikula, J. (2002). GTP-induced membrane binding and ion channel activity of annexin VI: Is annexin VI a GTP biosensor? *Biophysical Journal*, 82, 2737–2745, [https://doi.org/10.1016/S0006-3495\(02\)75614-2](https://doi.org/10.1016/S0006-3495(02)75614-2)
- Kirsch, T., Harrison, G., Golub, E. E., & Nah, H. D. (2000). The roles of annexins and types II and X collagen in matrix vesicle-mediated mineralization of growth plate cartilage. *Journal of Biological Chemistry*, 275, 35577–35583, <https://doi.org/10.1074/JBC.M005648200>
- Kuhn, L. T., Wu, Y., Rey, C., Gerstenfeld, L. C., Grynblas, M. D., Ackerman, J. L., Kim, H. M., & Glimcher, M. J. (2000). Structure, composition, and maturation of newly deposited calcium-phosphate crystals in chicken osteoblast cell cultures. *Journal of Bone and Mineral Research*, 15, 1301–1309, <https://doi.org/10.1359/JBMR.2000.15.7.1301>
- MacDonald, R. C., MacDonald, R. I., Menco, B. P. M., Takeshita, K., Subbarao, N. K., & Hu, L. R. (1991). Small-volume extrusion apparatus for preparation of large, unilamellar vesicles. *BBA - Biomembranes*, 1061, 297–303, [https://doi.org/10.1016/0005-2736\(91\)90295-J](https://doi.org/10.1016/0005-2736(91)90295-J)
- Margolis, H. C., Kwak, S. Y., & Yamazaki, H. (2014). Role of mineralization inhibitors in the regulation of hard tissue biomineralization: Relevance to initial enamel formation and maturation. *Frontiers in Physiology*, 5, article 339. 10.3389/FPHYS.2014.00339
- Marsh, D. (2008). Energetics of hydrophobic matching in lipid-protein interactions. *Biophysical Journal*, 94, 3996–4013, <https://doi.org/10.1529/BIOPHYSJ.107.121475>
- Mayer, L. D., Hope, M. J., & Cullis, P. R. (1986). Vesicles of variable sizes produced by a rapid extrusion procedure. *Biochimica et Biophysica Acta*, 858, 161–168, [https://doi.org/10.1016/0005-2736\(86\)90302-0](https://doi.org/10.1016/0005-2736(86)90302-0)
- Minashima, T., Small, W., Moss, S. E., & Kirsch, T. (2012). Intracellular modulation of signaling pathways by annexin A6 regulates terminal differentiation of chondrocytes. *Journal of Biological Chemistry*, 287, 14803–14815, <https://doi.org/10.1074/JBC.M111.297861>
- Parasassi, T., De Stasio, G., d'Ubaldo, A., & Gratton, E. (1990). Phase fluctuation in phospholipid membranes revealed by Laurdan fluorescence. *Biophysical Journal*, 57, 1179–1186, [https://doi.org/10.1016/S0006-3495\(90\)82637-0](https://doi.org/10.1016/S0006-3495(90)82637-0)
- Parasassi, T., De Stasio, G., Ravagnan, G., Rusch, R. M., & Gratton, E. (1991). Quantitation of lipid phases in phospholipid vesicles by the generalized polarization of Laurdan fluorescence. *Biophysical Journal*, 60, 179–186, [https://doi.org/10.1016/S0006-3495\(91\)82041-0](https://doi.org/10.1016/S0006-3495(91)82041-0)
- Plaut, J. S., Strzelecka-Kiliszek, A., Bozycki, L., Pikula, S., Buchet, R., Mebarek, S., Chadli, M., Bolean, M., Simao, A. M. S., Ciancaglini, P., Magrini, A., Rosato, N., Magne, D., Girard-Egrot, A., Farquharson, C., Esener, S. C., Millan, J. L., & Bottini, M. (2019). Quantitative atomic force microscopy provides new insight into matrix vesicle mineralization. *Archives of Biochemistry and Biophysics*, 667, 14–21, <https://doi.org/10.1016/J.ABB.2019.04.003>
- Raggatt, L. J., & Partridge, N. C. (2010). Cellular and molecular mechanisms of bone remodeling. *Journal of Biological Chemistry*, 285, 25103–25108, <https://doi.org/10.1074/jbc.R109.041087>
- Roberts, S., Narisawa, S., Harmey, D., Millán, J. L., & Farquharson, C. (2007). Functional involvement of PHOSPHO1 in matrix vesicle-mediated skeletal mineralization. *Journal of Bone and Mineral Research*, 22, 617–627, <https://doi.org/10.1359/jbmr.070108>
- Roberts, S. J., Stewart, A. J., Sadler, P. J., & Farquharson, C. (2004). Human PHOSPHO1 exhibits high specific phosphoethanolamine and phosphocholine phosphatase activities. *Biochemical Journal*, 382, 59–65, <https://doi.org/10.1042/BJ20040511>
- Simmer, J. P., & Fincham, A. G. (1995). Molecular mechanisms of dental enamel formation. *Critical Reviews in Oral Biology & Medicine*, 6, 84–108, <https://doi.org/10.1177/10454411950060020701>
- Sjöback, R., Nygren, J., & Kubista, M. (1995). Absorption and fluorescence properties of fluorescein. *Spectrochim. Acta Part A Mol. Biomol. Spectrosc.*, 51, L7–L21, [https://doi.org/10.1016/0584-8539\(95\)01421-P](https://doi.org/10.1016/0584-8539(95)01421-P)
- Smith, C. E., Chong, D. L., Bartlett, J. D., & Margolis, H. C. (2005). Mineral acquisition rates in developing enamel on maxillary and mandibular incisors of rats and mice: Implications to extracellular acid loading as apatite crystals mature. *Journal of Bone and Mineral Research*, 20, 240–249, <https://doi.org/10.1359/JBMR.041002>
- Smith, P. D., Davies, A., Crumpton, M. J., & Moss, S. E. (1994). Structure of the human annexin VI gene. *PNAS*, 91, 2713–2717, <https://doi.org/10.1073/PNAS.91.7.2713>
- Stechschulte, D. J., Morris, D. C., Silverton, S. F., Anderson, H. C., & Väänänen, H. K. (1992). Presence and specific concentration of carbonic anhydrase II in matrix vesicles. *Bone and Mineral*, 17, 187–191, [https://doi.org/10.1016/0169-6009\(92\)90734-U](https://doi.org/10.1016/0169-6009(92)90734-U)
- Tye, C. E., Sharma, R., Smith, C. E., & Bartlett, J. D. (2010). Altered ion-responsive gene expression in Mmp20 null mice. *Journal of Dental Research*, 89, 1421–1426, <https://doi.org/10.1177/0022034510384625>
- Veis, A., & Dorvee, J. R. (2013). Biomineralization mechanisms: A new paradigm for crystal nucleation in organic matrices. *Calcified Tissue International*, 93, 307–315, <https://doi.org/10.1007/S00223-012-9678-2>
- Veschi, E. A., Bolean, M., Strzelecka-Kiliszek, A., Bandorowicz-Pikula, J., Pikula, S., Granjon, T., Mebarek, S., Magne, D., Ramos, A. P., Rosato, N., Millán, J. L., Buchet, R., Bottini, M., & Ciancaglini, P. (2020). Localization of Annexin A6 in Matrix Vesicles During Physiological Mineralization. *International Journal of Molecular Sciences*, 21, 1367. 10.3390/IJMS21041367
- Wang, J., Yao, X., Liu, Y., Zhou, H., Chen, W., Sun, G., Su, J., Ma, X., & Tian, H. (2018). Vibration-Induced Emission: Tunable Photoluminescence Including White-Light Emission Based on Noncovalent Interaction-Locked N, N'-Disubstituted Dihydrodibenzo[a , c]phenazines (Advanced Optical Materials 12/2018). *Advanced Optical Materials*, 6, 1870049, <https://doi.org/10.1002/ADOM.201870049>
- Wuthier, R. E., Lipscomb, G. F., & Roy E Wuthier, G. F. L. (2011). Matrix vesicles: Structure, composition, formation and function in calcification. *Frontiers in Bioscience*, 16, 2812–2902, 10.2741/3887
- Zhang, Z., Sun, G., Chen, W., Su, J., & Tian, H. (2020). The endeavor of vibration-induced emission (VIE) for dynamic emissions. *Chemical Science*, 11, 7525–7537, <https://doi.org/10.1039/d0sc01591a>
- Zhou, H., Mei, J., Chen, Y.-A., Chen, C.-L., Chen, W., Zhang, Z., Su, J., Chou, P.-T., & Tian, H. (2016). Phenazine-based ratiometric Hg²⁺ probes with well-resolved dual emissions: A new sensing mechanism by vibration-induced emission (VIE). *Small*, 12, 6542–6546, <https://doi.org/10.1002/smll.201600731>

How to cite this article: Wang, Y., Weremiejczyk, L., Strzelecka-Kiliszek, A., Maniti, O., Amabile Veschi, E., Bolean, M., Ramos, A. P., Ben Trad, L., Magne, D., Bandorowicz-Pikula, J., Pikula, S., Millán, J. L., Bottini, M., Goekjian, P., Ciancaglini, P., Buchet, R., Dou, W. T., Tian, H., Mebarek, S., ... Granjon, T. (2022). Fluorescence evidence of Annexin A6 translocation across membrane in model matrix vesicles during apatite formation. *Journal of Extracellular Biology*, 1, e38. <https://doi.org/10.1002/jex2.38>